

# Surface and Image-Potential States on the $MgB_2(0001)$ Surfaces

V. M. Silkin<sup>1</sup>, E. V. Chulkov<sup>1,2</sup>, and P. M. Echenique<sup>1,2</sup>

<sup>1</sup>*Donostia International Physics Center (DIPC) and Centro Mixto CSIC-UPV/EHU, 20018 San Sebastián, Spain*

<sup>2</sup>*Departamento de Física de Materiales, Facultad de Ciencias Químicas, Universidad del País Vasco/Euskal Herriko Unibertsitatea, Apdo. 1072, 20018 San Sebastián/Donostia, Basque Country, Spain*

(October 28, 2018)

We present a self-consistent pseudopotential calculation of surface and image-potential states on  $MgB_2(0001)$  for both  $B$ -terminated ( $B-t$ ) and  $Mg$ -terminated ( $Mg-t$ ) surfaces. We find a variety of very clear surface and subsurface states as well as resonance image-potential states  $n=1,2$  on both surfaces. The surface layer DOS at  $E_F$  is increased by 55% at  $B-t$  and by 90% at the  $Mg-t$  surface compared to DOS in the corresponding bulk layers.

74.70.Ad, 73.20.At, 71.20.Lp

The discovery of the superconductivity in a simple metal polycrystalline compound  $MgB_2$  with the critical temperature  $T_c \sim 39$  K [1] has generated an explosion of research activity in studying the mechanism of the superconductivity and properties of this compound [2–25]. For instance, the superconductivity gap has been measured by both bulk sensitive methods [4,19] and surface sensitive techniques. Compared to bulk measurements the surface sensitive experiments, namely scanning tunneling spectroscopy (STS) [5–9] and point-contact experiments [10], give generally a smaller energy gap varying in the surface region [7,10]. It may be caused by two effects: surface contaminations or/and disorder and by changing the electronic structure at the surface. Qualitatively different STS spectra obtained by different groups on polycrystalline  $MgB_2$  pellets and films reflect different surface contaminations and microstructure of the sample surfaces. However, for a single crystal a possible change of a high density of states (DOS) at the Fermi level,  $E_F$ , high phonon frequencies and strong electron-phonon interactions can also lead to a change of the energy gap and  $T_c$  at the surface. Very recently two groups have announced obtaining single crystalline  $MgB_2$  with edge angles of 120 degrees [26,27]. These works open up new prospects for experimental studies of the surface superconductivity in  $MgB_2$ .

Due to strong covalent interactions within B planes [11,12,22,23] the (0001) termination of  $MgB_2$  is supposed to be more favorable. However nothing is known about atoms which form the topmost layer of  $MgB_2(0001)$ . The study of the (0001) termination of other metal diborides which also have crystal structures of the  $AlB_2$  type have shown that some metal diborides ( $TiB_2$ ,  $HfB_2$ ) are terminated by metal atoms [28,29] while the topmost layer of  $TaB_2$  is formed by the graphitic boron layer [30]. Here we report on *ab initio* calculations of the electronic structure of the  $MgB_2(0001)$  surface for both types of termination. In order to assess the effect of the surface relaxation on surface states we have computed the surface electronic structure for the ideally bulk terminated crystal as well as for contracted and expanded by 6% the first

interlayer spacing.

The bulk electronic structure of  $MgB_2$  [11,12,22,23] leads to an unconventional bulk states projection with very wide absolute and symmetry energy gaps (Fig. 1) which support a variety of surface states and give an additional contribution to crystal reflectivity at energy interval just below the vacuum level where resonance image-potential states arise. The surface and image states are of crucial importance for the description of the surface dynamical screening, electron (hole) excitations, and superconductivity at  $MgB_2$  surfaces. We show that for the  $Mg$ -terminated ( $Mg-t$ ) surface the surface states contribution nearly doubles the surface DOS at  $E_F$  compared to the bulk  $Mg$  layer DOS. For the  $B$ -terminated ( $B-t$ ) surface the surface state contribution increases the surface DOS at  $E_F$  by 55% compared to that in bulk. Special attention in the paper is focused on image potential states. We find that  $Mg$ - and  $B$ -layers possess distinct reflectivity that leads to different localization of image state wave function in bulk region.

The calculations of charge density have been performed within the self-consistent local density-functional plane-wave method by using a supercell of 13 atomic layers and 7 layers of vacuum [31]. This supercell is big enough to ensure a good description of both surface and bulk states. Experimental values of lattice constants  $a = 5.8317$  a.u. and  $c = 6.6216$  a.u. used in the evaluation have been taken from Ref. [1]. The 13 layer slab representing the  $B-t$  ( $Mg-t$ ) surface consists of 7  $B(Mg)$  layers alternating with 6  $Mg(B)$  layers.

As the LDA potential does not describe the correct asymptotic potential behavior in the vacuum region we modify it by retaining the self-consistent LDA one for  $z < z_{im}$ , where  $z_{im}$  is the image plane position, and replacing it in the vacuum region for  $z > z_{im}$  by  $V(z) = \{exp[-\lambda(z - z_{im})] - 1\}/[4(z - z_{im})]$ . The damping parameter  $\lambda$  is a function of  $(x, y)$  and is fixed by the requirement of continuity of the potential at  $z = z_{im}$  for each couple of  $(x, y)$ . With the use of the self-consistent charge density obtained for a 13-layer slab we have constructed charge density for a 31-layer slab inserting 18

bulk layers into the center of the slab. Vacuum space was increased from 7 layers to 21 ones. This vacuum interval is enough to accurately describe the  $n=1$  and 2 image states. Finally the LDA potential was generated for this new supercell with a correct image tail in vacuum space.

In Figs.1a and 1b we show the calculated projection of bulk band structure onto the surface Brillouin zone together with surface states for  $B-t$  and  $Mg-t$  surfaces, respectively. The light grey areas show the  $\pi$  projected bulk states and the grey ones indicate the  $\sigma$  states. A remarkable feature of the bulk states projection is the presence of two wide absolute energy gaps. The lower gap separates the  $s$ -bulk bands and  $p_z$  bands of boron, the upper gap crossed by the  $p_{x,y}$  bulk bands of  $B$  is located in the vicinity of the Fermi level,  $E_F$ . The  $B-t$  surface (Fig.1a) has 4 surface states strongly localized in the topmost boron layer and 3 subsurface states. All these states show energy dispersion which repeats that of bulk bands. Two surface states degenerated at the  $\bar{\Gamma}$  point are of the  $p_{x,y}$  symmetry ( $\sigma$  states). They split off from bulk states of the same symmetry by 0.45 eV and have energy of 1.23 eV relative to  $E_F$ . Their charge density is completely localized in the topmost layer (Fig.2). One can consider these states as two-dimensional quantum-well states due to their extremely strong localization in the  $z$  direction: they decay into the bulk much faster than do conventional surface states which are characterized by a smooth exponential decay. Another surface state with energy of -2.74 eV is of the  $p_z$  symmetry ( $\pi$  state), 75% of the state is concentrated in the three surface atomic layers and in the vacuum region (Fig.3). The lower surface state is of  $s$  symmetry and splits off from bulk states by 0.4 eV, 70% of the state is localized in the topmost layer. The subsurface states with energy of 0.35 eV degenerated at  $\bar{\Gamma}$  are localized in a few subsurface  $B$  layers with 40% of the state concentrating in the second  $B$  layer. The third subsurface state is located at the bottom of the  $s$  bulk boron states.

The  $Mg-t$  surface shows distinct electronic structure compared to the  $B-t$  one. In particular, the  $Mg$  occupied surface state of the  $s-p_z$  symmetry with energy of -1.94 eV appears at the  $\bar{\Gamma}$  point. Its charge density distribution localized mostly (65%) in the  $Mg$  surface layer and in the vacuum region is shown in Fig.4. The origin of this state can be understood from a simple charge transfer picture. In bulk the  $Mg$  atom donates two valence electrons to the adjacent  $B$  planes thus moving up to  $E > E_F$  all the  $Mg$  bands. In the surface layer the  $Mg$  atom donates one electron to the subsurface  $B$  plane while another electron forms the dangling bond ( $s-p_z$ ) occupied surface state.

Unoccupied subsurface states with energy of 0.36 eV degenerated at  $\bar{\Gamma}$  are formed by the subsurface  $B$  layer, 70% of the state is concentrated in the layer. At energy  $\sim -12.3$  eV there also exists a subsurface resonance state

generated by the  $B$  layers.

In Fig.5 we show the calculated surface layer DOS for both the  $B-t$  and  $Mg-t$  surfaces and compare them with the corresponding central layer DOS. In the  $B-t$  surface the surface DOS at  $E_F$  which also includes the vacuum region is by 55% higher than the central  $B$  layer DOS. In the  $Mg-t$  surface the surface DOS at  $E_F$  is higher than the central  $Mg$  layer DOS by factor of 2. Both these results favour the higher surface critical temperature  $T_c^s$  compared to that in bulk.

It is less known about phonons on the  $MgB_2(0001)$  surface. There normally exist surface phonon modes on metal surfaces with slightly smaller frequencies compared to those in bulk [32]. In bulk  $MgB_2$  the in-plane boron mode  $E_{2g}$  is responsible for strong electron-phonon interaction [13,25]. Because of its in-plane character one can expect that the vibrational frequencies and atomic displacements of this mode in the surface or subsurface boron layer will be similar to those in bulk. Therefore one can expect very similar or even higher  $T_c^s$  compared to  $T_c$ .

Image states fall in a group of surface states which are linked to the vacuum level and located relatively far from the surface. The calculated work function which fixes the vacuum level relative to  $E_F$  was obtained to be of 6.1 eV for the  $B-t$  surface and 4.2 for the  $Mg-t$  one. Similar to simple and noble metal surfaces [33] the wave function maximum of the  $n=1$  image state on  $MgB_2$  is located at  $\sim 6$  a.u. beyond the surface atomic layer for both surfaces. In Figs.1a and 1b we show the calculated  $n=1,2$  resonance image states. Nothing is known about the image plane position on  $MgB_2$  and we varied  $z_{im}$  for both terminations within the 2.0-3.5 a.u. interval beyond the surface layer. This variation leads to  $E_1 = -0.9 \pm 0.15$  eV and  $E_2 = -0.25 \pm 0.05$  eV for the  $B-t$  surface as well as to  $E_1 = -1.1 \pm 0.15$  eV and  $E_2 = -0.30 \pm 0.05$  eV for the  $Mg-t$  surface, the error bar includes the energy dependence on the  $z_{im}$  position. The energies obtained are rather similar to those for the  $n=1,2$  resonance image states on simple metal surfaces [33].

The resonance image states are mostly degenerated with magnesium bulk states. The interaction between the image states and the  $Mg$  bulk states results in a different reflectivity of  $B$  and  $Mg$  layers and a different behavior of the image state wave functions in bulk. The amplitude of these wave functions is significantly larger in magnesium layers than in boron ones. This behavior of image states is specific for  $MgB_2$  due to its peculiar bulk electronic structure and was not found for simple and noble metals [33].

It is known that the relaxation of closed-packed simple metal surfaces [34] is relatively small: the contraction/expansion of the first interlayer spacing is  $\leq 6\%$ . We have inspected the dependence of the surface electronic structure by computing slabs with the contracted and expanded first interlayer spacing by 6% for both ter-

minations. We have found that these relaxations lead to change of the surface state energies within 0.1 eV and to small change of the surface DOS at  $E_F$ . The change of the  $n=1,2$  image state energies is significantly smaller than the error bar.

In conclusion, we have performed self-consistent pseudopotential calculations of the surface electronic structure for the  $B-t$  and  $Mg-t$  surfaces of  $MgB_2$ . We have found a variety of surface and subsurface states as well as two resonance image states on both surfaces including an unoccupied quantum well state of the  $p_{x,y}$  symmetry on the  $B-t$  surface. Due to very clear surface character of these states the  $MgB_2(0001)$  surfaces provide good opportunity to test the theoretical results by measuring the surface electronic structure by different spectroscopies such as photoemission, inverse photoemission, time-resolved two-photon photoemission, and scanning tunneling spectroscopy. The obtained higher surface layer DOS at  $E_F$  favours the higher critical temperature compared to that in bulk. This is inconsistent with recent STS experiments which have shown an opposite trend [5–9]. We attribute this discrepancy to contaminations and disorder on polycrystal sample surfaces.

We acknowledge support by the Basque Country University, Basque Hezkuntza Saila, and Iberdrola S.A.

---

[1] J. Nagamatsu *et al.*, Nature **410**, 63 (2001).  
[2] S. L. Bud'ko *et al.*, Phys. Rev. Lett. **86**, 1877 (2001).  
[3] D. K. Finnemore *et al.*, Phys. Rev. Lett. **86**, 2420 (2001).  
[4] T. Takahashi *et al.*, Phys. Rev. Lett. **86**, 4915 (2001).  
[5] G. Rubio-Bollinger, H. Suderow, and S. Vieira, cond-mat/0102242.  
[6] G. Karapetrov *et al.*, Phys. Rev. Lett. **86**, 4374 (2001).  
[7] F. Giubileo *et al.*, cond-mat/0105146.  
[8] C. -T. Chen *et al.*, cond-mat/0104285.  
[9] A. Sharoni, I. Felner, and O. Millo, Phys. Rev. B **63**, 220508R (2001).  
[10] H. Schmidt *et al.*, cond-mat/0102389.  
[11] J. Kortus *et al.*, Phys. Rev. Lett. **86**, 4656 (2001).  
[12] J. M. An and W. E. Pickett, Phys. Rev. Lett. **86**, 4366 (2001).  
[13] Y. Kong *et al.*, Phys. Rev. B **64**, 020501R (2001).  
[14] J. E. Hirsch and F. Marsiglio, cond-mat/0102479.  
[15] K. Voelker, V. I. Anisimov, and T. M. Rice, cond-mat/0103082.  
[16] R. Osborn *et al.*, cond-mat/0103064.  
[17] E. Bascones and F. Guinea, cond-mat/0103190.  
[18] A. Y. Liu, I. I. Mazin, and J. Kortus, cond-mat/0103570.  
[19] B. Gorshunov *et al.*, cond-mat/0103164.  
[20] J. D. Jorgensen, D. G. Hinks, and S. Short, cond-mat/0103069.  
[21] E. Saito *et al.*, J. Phys.:Condens. Matter, **13**, L267 (2001).

[22] K. D. Belashchenko, M. van Schilfgaarde, and V. P. Antropov, con-mat/0102290.  
[23] G. Satta *et al.*, cond-mat/0102358.  
[24] T. J. Sato, K. Shibata, and Y. Takano, cond-mat/0102468.  
[25] K. P. Bohnen, R. Heid, and B. Renker, cond-mat/0103319.  
[26] C. U. Jung *et al.*, cond-mat/0105330.  
[27] M. Xu *et al.*, cond-mat/0105271.  
[28] W. Hayami *et al.*, Jpn. J. Appl. Phys. **10**, 172 (1994).  
[29] C. L. Perkins *et al.*, Surf. Sci. **470**, 215 (2000).  
[30] H. Kawanowa *et al.*, Phys. Rev. Lett. **81**, 2264 (1998).  
[31] The Be pseudopotential is generated according to N. Troullier and J. L. Martins, Phys. Rev. B **43**, 1993 (1991). The exchange-correlation potential is obtained within LDA (J. P. Perdew and A. Zunger, Phys. Rev. B **23**, 5048 (1981)). Convergent results for energy spectrum within 0.02 eV were obtained with a 25 Ry plane-wave cut-off for the wave functions and a 18x18 special  $k_{||}$  sampling points.  
[32] J. B. Hannon, E. J. Mele, and E. W. Plummer, Phys. Rev. B **53**, 2090 (1996).  
[33] E. V. Chulkov, V. M. Silkin, and P. M. Echenique, Surf. Sci. **437**, 330 (1999); V. M. Silkin, E. V. Chulkov, and P. M. Echenique, Phys. Rev. B **60**, 7820 (1999).  
[34] Ph. Hofmann *et al.*, Phys. Rev. B **53**, 13715 (1996).

FIG. 1. Projected bulk band structure of  $MgB_2$  together with the surface and image-potential states for  $B$ -terminated (a) and  $Mg$ -terminated (b) surfaces. The light (dark) grey areas represent the  $\pi$  ( $\sigma$ ) projected bulk states. Dotted areas indicate the magnesium projected states. Thick solid lines depict surface state which are mostly localized in the topmost  $B$  layer.

FIG. 2. Charge density distribution of the unoccupied boron surface (quantum well) state at  $\Gamma$  in the  $(10\bar{1}0)$  plane for the  $B$ -terminated surface. Small (large) filled circles indicate the  $B$  ( $Mg$ ) atom positions.

FIG. 3. Charge density distribution of the occupied boron  $p_z$  surface state at  $\Gamma$  in the  $(10\bar{1}0)$  plane for the  $B$ -terminated surface.

FIG. 4. Charge density distribution of the occupied magnesium  $p_z$  surface state at  $\Gamma$  in the  $(10\bar{1}0)$  plane for the  $Mg$ -terminated surface.

FIG. 5. The calculated surface layer DOS at  $E_F$  (solid lines) for both  $B$ - and  $Mg$ -terminated surfaces. Dashed lines show the difference between the surface layer DOS and the corresponding central layer DOS.

Fig. 1a

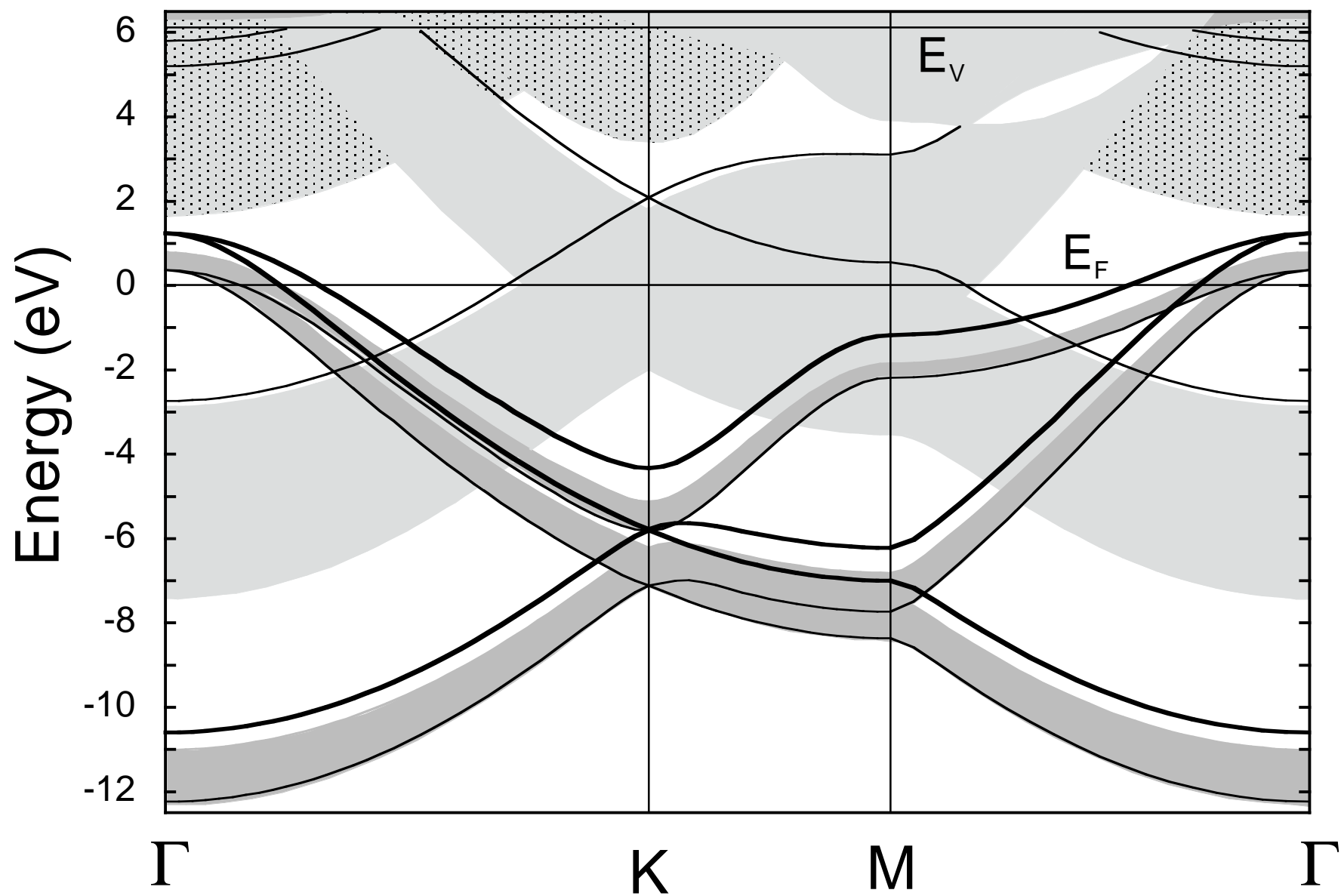


Fig. 1b

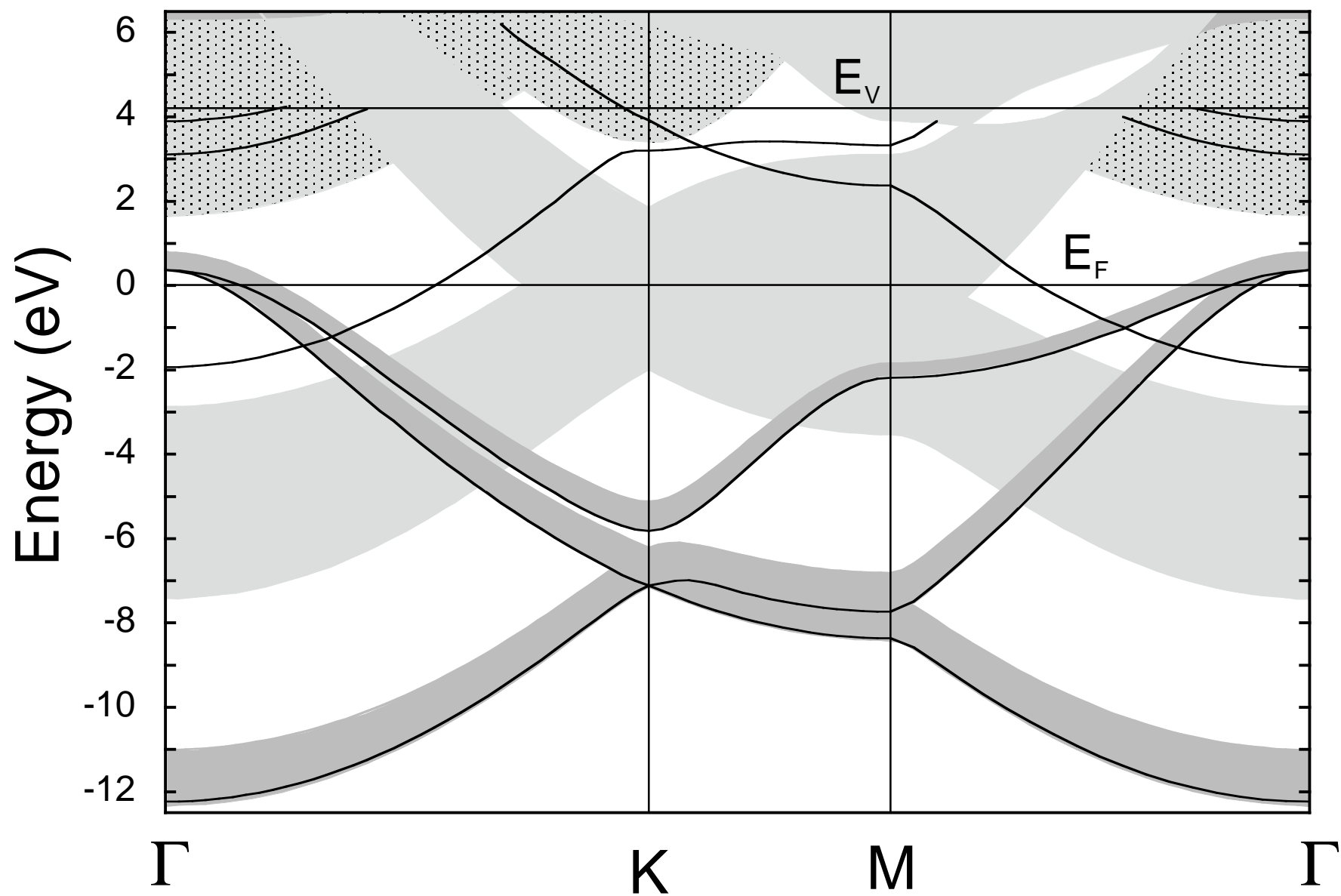


Fig.2

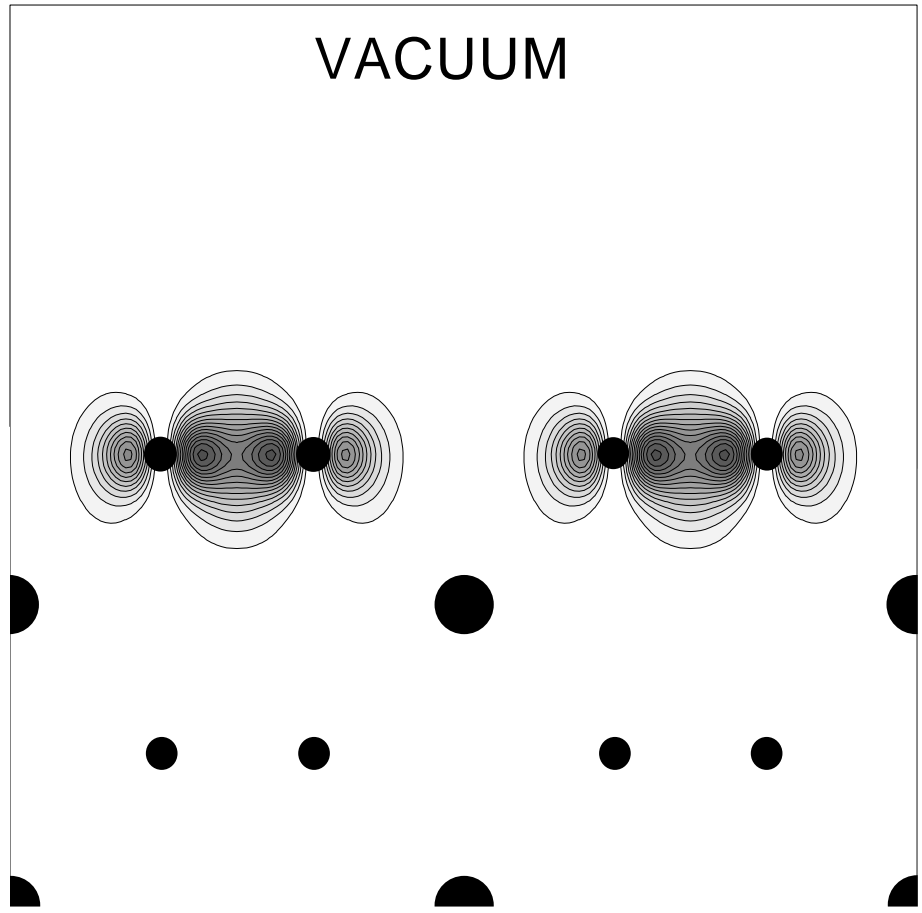


Fig.3

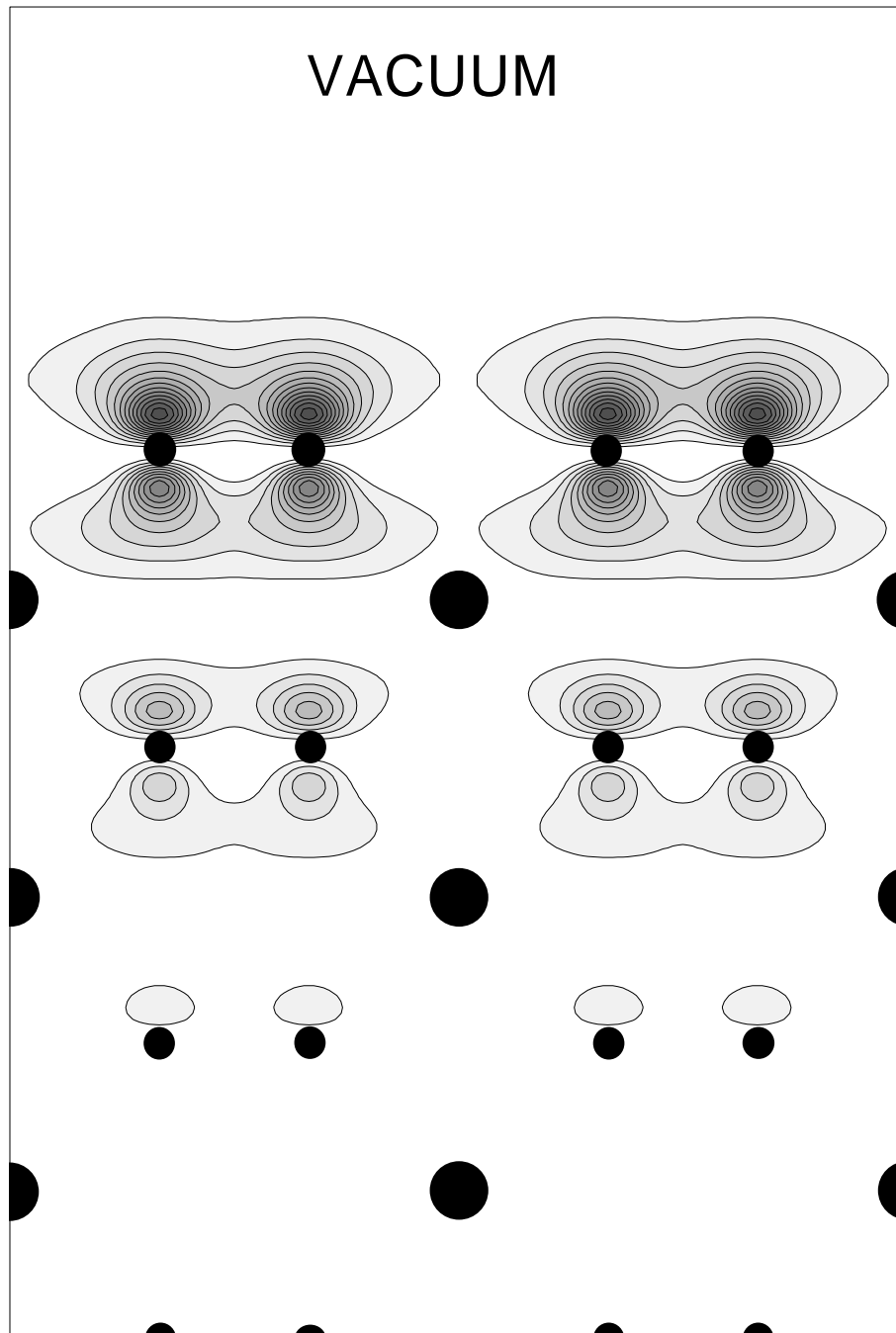


Fig. 4

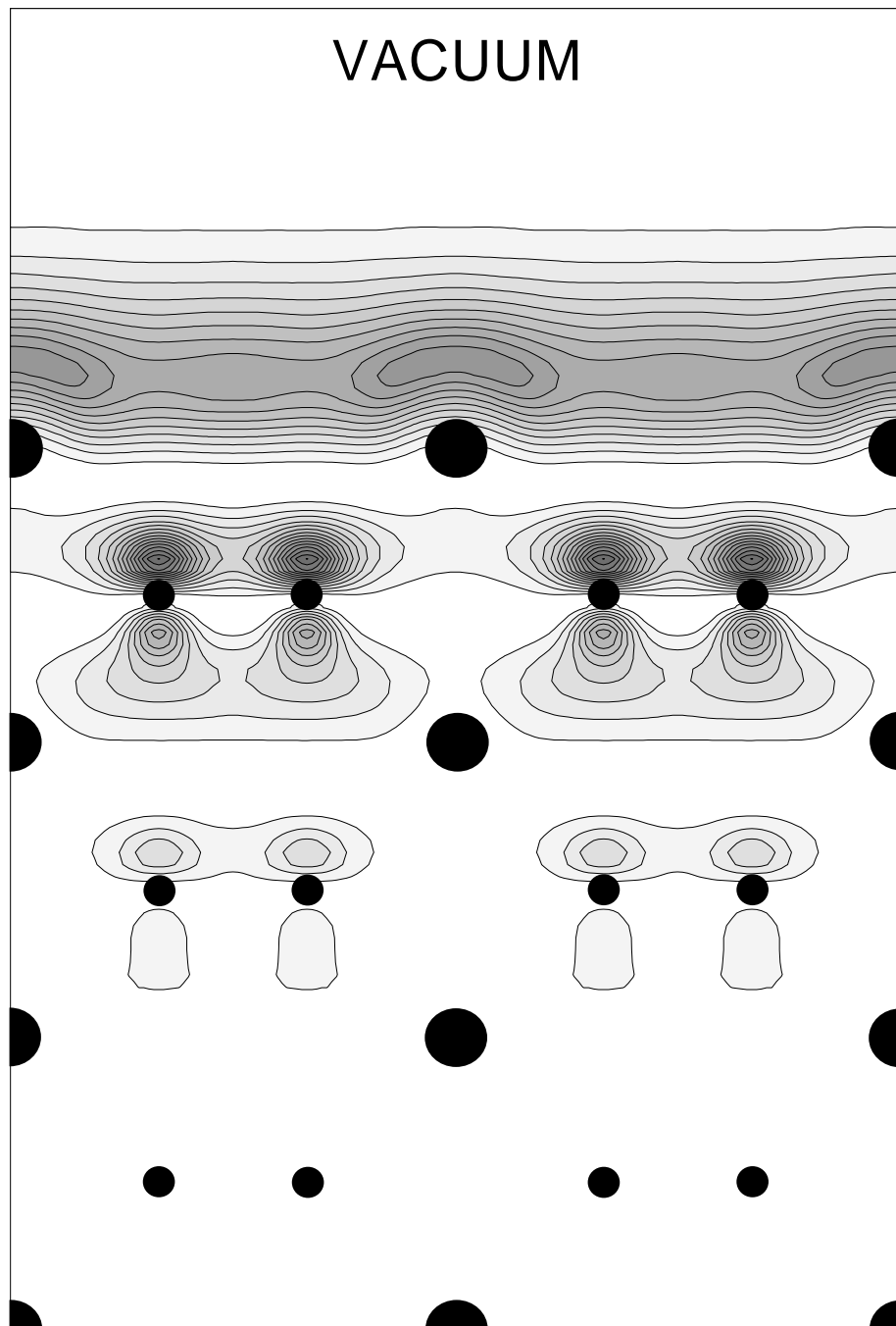




Fig. 5

